Receptor interacting protein kinase mediates necrotic cone but not rod cell death in a mouse model of inherited degeneration

Receptor interacting protein kinase mediates necrotic cone but not rod cell death in a mouse model of inherited degeneration

Yusuke Murakami[a], Hidetaka Matsumoto[a], Miin Roh[a], Jun Suzuki[a], Toshio Hisatomi[b], Yasuhiro Ikeda[b], Joan W. Miller[a], and Demetrios G. Vavvas[a,1]

[a]Retina Service, Angiogenesis Laboratory, Massachusetts Eye and Ear Infirmary, Department of Ophthalmology, Harvard Medical School, Boston, MA 02114; and [b]Department of Ophthalmology, Graduate School of Medical Sciences, Kyushu University, Fukuoka 812-8582, Japan

Edited* by Patricia K. Donahoe, Massachusetts General Hospital, Boston, MA, and approved July 27, 2012 (received for review April 24, 2012)

Retinitis pigmentosa comprises a group of inherited retinal photoreceptor degenerations that lead to progressive loss of vision. Although in most cases rods, but not cones, harbor the deleterious gene mutations, cones do die in this disease, usually after the main phase of rod cell loss. Rod photoreceptor death is characterized by apoptotic features. In contrast, the mechanisms and features of subsequent nonautonomous cone cell death remain largely unknown. In this study, we show that receptor-interacting protein (RIP) kinase mediates necrotic cone cell death in *rd10* mice, a mouse model of retinitis pigmentosa caused by a mutation in a rod-specific gene. The expression of RIP3, a key regulator of programmed necrosis, was elevated in *rd10* mouse retinas in the phase of cone but not rod degeneration. Although *rd10* mice lacking *Rip3* developed comparable rod degeneration to control *rd10* mice, they displayed a significant preservation of cone cells. Ultrastructural analysis of *rd10* mouse retinas revealed that a substantial fraction of dying cones exhibited necrotic morphology, which was rescued by *Rip3* deficiency. Additionally, pharmacologic treatment with a RIP kinase inhibitor attenuated histological and functional deficits of cones in *rd10* mice. Thus, necrotic mechanisms involving RIP kinase are crucial in cone cell death in inherited retinal degeneration, suggesting the RIP kinase pathway as a potential target to protect cone-mediated central and peripheral vision loss in patients with retinitis pigementosa.

apoptosis | neurodegeneration | neuroprotection | oxidation | inflammation

Retinitis pigmentosa (RP) refers to a group of inherited retinal degenerations that affect over one million individuals globally (1). Although vitamin A supplementation and an ω-3 rich diet has been shown to slow down the visual decline in some patients (2), they do not stop the disease progression and irreversible vision loss still ensues for many patients. Vision loss in RP results from photoreceptor cell death and typically begins with loss of night vision (because of rod dysfunction and death), followed by loss of peripheral and central vision because of loss of cones. This cone-mediated dysfunction is the most debilitating aspect of the disease for patients. Molecular genetic studies have identified mutations in more than 50 genes, most expressed exclusively in rod photoreceptors, which are associated with RP. Although rods that harbor the deleterious gene mutations are expected to die, it is still a puzzle why and how cones—that do not harbor deleterious gene mutations—do die subsequent to the rod degeneration phase.

Apoptosis and necrosis are two distinct modes of cell death defined by morphological appearance (3). Apoptosis is the best-characterized type of programmed cell death, and the caspase family proteases play a central role in the induction of this process (4). Necrosis, which was traditionally thought to be an uncontrolled process of cell death, is now known to also have a regulated component in some instances (5, 6). Two members of the receptor-interacting protein (RIP) kinase family proteins, RIP1 and RIP3, have been identified as critical mediators of programmed necrosis (7). RIP1 is a multifunctional death-domain adaptor protein that mediates both apoptosis and necrosis. RIP1 induces apoptosis when recruited to the protein complex containing Fas-associated death domain and caspase-8 (8, 9). When caspases are either inhibited or not activated, RIP1 binds with RIP3 to form a pronecrotic complex, which is stabilized by phosphorylation of their serine/threonine kinase domains (10–12). RIP kinase-dependent necrosis has been implicated in various forms of developmental and pathological cell death (13–18). However, studies on RIP kinase in the central nervous system have been restricted to acute models of neuronal demise (19–21), and its roles in neurodegenerative diseases caused by genetic mutations remain largely unexplored.

In animal models of RP, rod cell death has been shown to occur through apoptosis (22). However, attempts to inhibit caspases by pharmacologic or genetic interventions have failed to show effective protection against rod cell apoptosis (23, 24). Recent studies have demonstrated that caspase-independent molecules, such as calpains and poly(ADP ribose) polymerases, which mediate not only apoptosis but also necrosis, are activated during rod cell death (25, 26). The mechanisms of cone cell death in RP are less well characterized. Although loss of rod-derived trophic factors (27), oxidative stress (28), and nutrient starvation (29) are shown to contribute to the cone degeneration, little is known about the cell death types and molecules that mediate cone cell death.

The present study investigates a possible role for RIP kinase and necrosis in *rd10* mice, a model of RP caused by a mutation in the rod-specific gene that encodes rod cGMP phosphodiesterase β-subunit (*Pde6β*) (30). The data identify RIP kinase-mediated necrosis as a mechanism of cone cell death in rod-initiated retinal degeneration and as a potential therapeutic target.

Results

Increased RIP3 and RIP1 Expression in the Late Phase of Retinal Degeneration in *Rd10* Mice. RIP3 is a key regulator of RIP1 kinase activation (7), and its expression level correlates with the responsiveness to programmed necrosis (11). We first investigated the changes in RIP3 and RIP1 expression in the retinas of *rd10* mice, an animal model of RP caused by a missense mutation in exon 13 of the rod-specific *Pde6β* gene (30). Mutations in this gene have been found in patients with autosomal recessive RP (31). *Rd10* mice develop progressive rod degeneration beginning around postnatal day 18 (P18); only one to three rows of

Author contributions: Y.M., J.W.M., and D.G.V. designed research; Y.M., H.M., M.R., J.S., T.H., and Y.I. performed research; Y.M., H.M., M.R., J.S., T.H., Y.I., J.W.M., and D.G.V. analyzed data; and Y.M., J.W.M., and D.G.V. wrote the paper.

Conflict of interest statement: The Massachusetts Eye and Ear Infirmary Institution has filed patents on the subject of neuroprotection in retinal degenerations. Y.M., J.W.M., and D.G.V. are named inventors.

*This Direct Submission article had a prearranged editor.

[1]To whom correspondence should be addressed. E-mail: demetrios_vavvas@meei.harvard.edu.

This article contains supporting information online at www.pnas.org/lookup/suppl/doi:10.1073/pnas.1206937109/-/DCSupplemental.

photoreceptors remain at P28, and cone degeneration follows (32). Therefore, we chose P21 and P28 as time points for rod cell death, and P35, P42, and P56 as time points for cone cell death in the following experiments. Quantitative real-time PCR showed that RIP3 mRNA expression levels did not change at P21, but increased fourfold at P35 in *rd10* mouse retinas compared with those of age-matched WT controls ($P < 0.01$) (Fig. 1*A*). RIP1 expression was also elevated threefold in the retinas of P35 *rd10* mice ($P < 0.01$) (Fig. 1*B*). Western blot confirmed that RIP3 and RIP1 protein expression increased in P35 *rd10* mouse retinas compared with that in WT retinas ($P < 0.05$) (Fig. 1*C*). These data suggest that the RIP kinase pathway may be activated during retinal degeneration of *rd10* mice, especially in the late phase of photoreceptor cell death.

RIP Kinase Has a Minor Role in Rod Degeneration of *Rd10* Mice. To assess the function of RIP kinase in inherited retinal degeneration, we crossed *rd10* mice with *Rip3* knockout mice (33) to generate *rd10*;*Rip3*$^{-/-}$ mice. We first examined the rod cell death kinetics in these animals. TUNEL staining showed that the number of TUNEL-positive cells in the outer nuclear layer (ONL) did not change in *rd10*;*Rip3*$^{-/-}$ mice compared with control *rd10*;*Rip3*$^{+/+}$ mice at P21 (Fig. 2 *A* and *B*). To evaluate the photoreceptor cell loss, we measured ONL thickness at six points along the horizontal meridian of the eye. There was no significant difference in ONL thickness between *rd10*;*Rip3*$^{-/-}$ and *rd10*;*Rip3*$^{+/+}$ mice at P21 (Fig. 2*C*). The ONL was reduced to one to three rows of photoreceptor nuclei in both genotypes at P28 (Fig. 2 *D* and *E*). These results indicate that inhibition of RIP kinase alone is not sufficient to prevent rod cell loss in *rd10* mice. Because RIP kinase and caspase function redundantly to induce cell death in several conditions (34), we next examined whether combined targeting of RIP kinase and caspase protects rod photoreceptors against cell death in *rd10* mice. To address this question, we treated *rd10*;*Rip3*$^{-/-}$ mice with the pan-caspase inhibitor IDN-6556 (10 mg·kg·d) using an osmotic pump from P21 to P28. However, the pan-caspase inhibitor provided no protective effect against rod cell loss in *rd10*;*Rip3*$^{-/-}$ mice compared with vehicle treatment at P28 (Fig. S1 *A* and *B*). Correspondingly, combined treatments with the pan-caspase inhibitor and the RIP1 kinase inhibitor necrostatin-1 (Nec-1) (15 mg·kg·d) (35) did not prevent rod cell loss in *rd10* mice (Fig. S1 *C* and *D*).

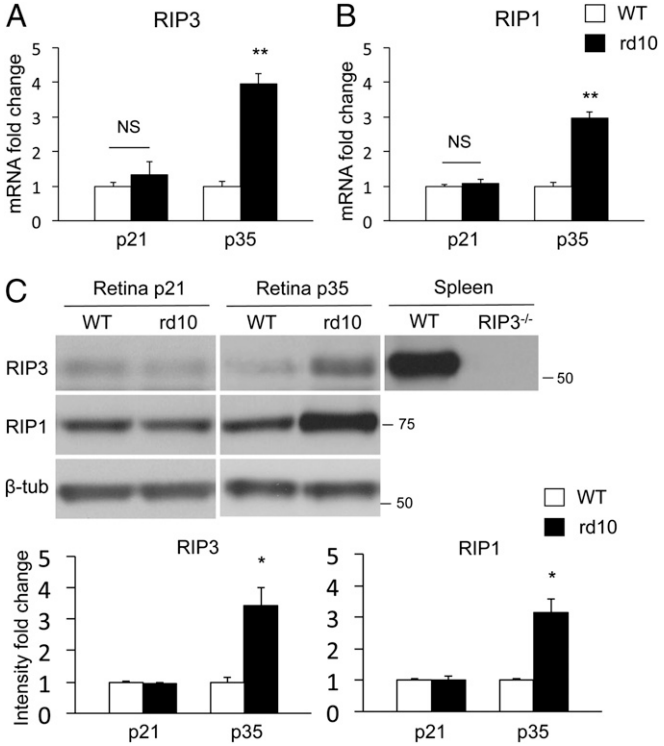

Fig. 1. Increased RIP3 and RIP1 expression in the late phase of retinal degeneration in *rd10* mice. (*A* and *B*) Quantitative real-time PCR analysis for RIP3 (*A*) and RIP1 (*B*) in WT and *rd10* retinas at P21 and P35 (n = 5–7 each). $^{**}P < 0.01$. (*C*) Western blot analysis for RIP3 and RIP1 at P21 and P35 of WT and *rd10* retinas (n = 4 each). Levels normalized to β-tubulin. For RIP3 analysis, spleen samples from WT and *Rip3*$^{-/-}$ animals were used as positive and negative controls, respectively. The bar graphs indicate the relative level of RIP3 and RIP1 to β-tubulin by densitometric analysis. $^{*}P < 0.05$.

Rod Photoreceptor Cell Death in *Rd10* Mice Is Mainly Caused by Apoptosis. Although TUNEL staining was initially thought to detect apoptotic cells specifically, several studies have demonstrated that TUNEL also labels DNA breaks in necrotic cells (36, 37). Therefore, it is difficult to discriminate between apoptosis and necrosis by TUNEL assay alone. To analyze further the types of rod cell death, we investigated the morphology of photoreceptors by transmission electron microscopy (TEM). Consistent with previous studies showing apoptosis in animal models of RP (22, 38), most of the dying rod photoreceptors were associated with apoptotic morphology, such as nuclear condensation and cellular shrinkage in P21 *rd10* mouse retinas (Fig. 3 *A* and *F*). Necrotic photoreceptor cell death was rarely observed at this time point (Fig. 3 *B* and *F*). The mitochondrial structure of the inner segment of photoreceptors was well preserved (Fig. 3*C*). There was no significant morphological difference of rod cell death between *rd10*;*Rip3*$^{-/-}$ and *rd10*;*Rip3*$^{+/+}$ mice (Fig. 3 *D*–*F*). Collectively, these findings support that the RIP kinase pathway is not important for apoptotic rod cell death in *rd10* mice.

RIP Kinase Deficiency Rescues Cone Photoreceptor Cell Death in *Rd10* Mice. We next evaluated the role of RIP kinase in cone degeneration of *rd10* mice. TUNEL staining in P35 *rd10* mouse retinas showed that the appearance of TUNEL-positive photoreceptor nuclei was significantly decreased by *Rip3* deficiency (P = 0.0062) (Fig. 4 *A* and *B*). To assess the cone cell loss, we performed whole-mount immunofluorescence for peanut agglutinin lectin (PNA), which selectively binds to cone inner and outer segments (39). At P21, the cone cell density of *rd10* mice was comparable to that of WT mice, although the length of inner and outer segments was relatively shortened in *rd10* mice (Fig. S2). No difference in cone cell density was observed by *Rip3* deficiency at P21 (Fig. S2). Thereafter, the cones in *rd10* mice were gradually lost by P42, with a further decrease between P42 and P56 (Fig. 4 *C*–*F*). In contrast, *rd10*;*Rip3*$^{-/-}$ mice retained substantially more cones at both P42 and P56, compared with the age-matched *rd10*;*Rip3*$^{+/+}$ mice ($P <$ 0.01) (Fig. 4 *C*–*F*). We also assessed the effect of *Rip3* deficiency on cone function by measuring photopic electroretinogram (ERG). The b-wave amplitude in the eyes of *rd10*;*Rip3*$^{-/-}$ mice was significantly higher than those of *rd10*;*Rip3*$^{+/+}$ mice (P = 0.0022) (Fig. 4 *G* and *H*). Thus, *Rip3* deficiency provides histological and functional rescue of cone photoreceptors in *rd10* mice.

Consistent with the data from genetic *Rip3* ablation, pharmacologic treatment with a systemic and continuous delivery of Nec-1 retained a twofold higher number of cone cells in *rd10* mice compared with treatment with vehicle (P = 0.0105) (Fig. 5 *A* and *B*). In addition, Nec-1 treatment partially prevented the reduction in photopic b-wave amplitude in *rd10* mice compared with vehicle treatment (P = 0.0494) (Fig. 5 *C* and *D*). Collectively, these data indicate that RIP kinase plays an important role in cone cell death in *rd10* mice.

Cone Photoreceptor Cell Death in *Rd10* Mice Is Associated with Necrotic Features. We further analyzed the morphological changes during cone degeneration by TEM. In P35 *rd10* mice, the photoreceptors, which were predominantly composed of cones, showed cellular swelling in the inner segments (Fig. 6*A*). The ONL contained not only apoptotic nuclei, but also necrotic cells accompanied by cytoplasmic swelling and plasma membrane rupture (Fig. 6

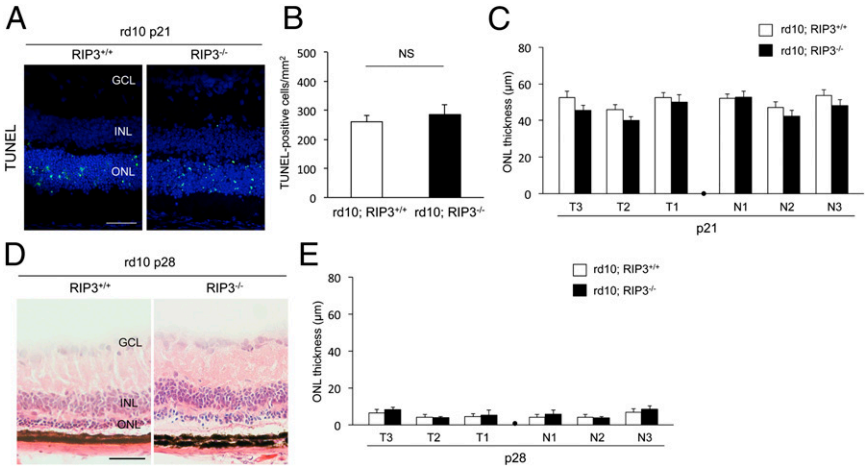

Fig. 2. *Rip3* deficiency does not prevent rod photoreceptor degeneration in *rd10* mice. (*A*) TUNEL (green) and DAPI (blue) staining at P21 of *rd10*;*Rip3*$^{+/+}$ and *rd10*;*Rip3*$^{-/-}$ mice. GCL, ganglion cell layer; INL, inner nuclear layer; ONL, outer nuclear layer. (Scale bar, 50 μm.) (*B* and *C*) Quantification of TUNEL-positive photoreceptors (*B*) and ONL thickness (*C*) at P21 of *rd10*;*Rip3*$^{+/+}$ and *rd10*;*Rip3*$^{-/-}$ mice (n = 6 each). NS, not significant. T3–T1: retinal thickness at 1,200 μm, 800 μm, and 400 μm from the optic nerve in the temporal hemisphere. N1–N3: retinal thickness at 400 μm, 800 μm, and 1,200 μm from the optic nerve in the nasal hemisphere. There was no significant difference in either TUNEL-positive cells or ONL thickness between *rd10*;*Rip3*$^{+/+}$ and *rd10*;*Rip3*$^{-/-}$ mice. (*D* and *E*) Retinal histology (*D*) and quantification of ONL thickness (*E*) at P28 of *rd10*; *Rip3*$^{+/+}$ and *rd10*; *Rip3*$^{-/-}$ mice (n = 6 each). (Scale bar, 50 μm.) No significant difference was observed between *rd10*; *Rip3*$^{+/+}$ and *rd10*;*Rip3*$^{-/-}$ mice.

B and *G*). The mitochondria in the inner segments were frequently associated with swelling and membrane rupture, which are characteristics of necrosis (Fig. 6*C*). In contrast, the number of necrotic photoreceptors was significantly decreased in *rd10*;*Rip3*$^{-/-}$ mice ($P < 0.05$) (Fig. 6 *D*–*G*). These findings demonstrate that necrosis is involved in cone degeneration, and that RIP kinase is critical for the necrotic cone cell death in *rd10* mice.

RIP Kinase Deficiency Reduces Oxidative Stress in *Rd10* Mice. Oxidative damage has been implicated in cone cell death in animal models of RP, including *rd10* mice (40). Because RIP kinase promotes necrosis via reactive oxygen species (ROS) overproduction in several types of cells (10, 13, 41), we next examined the effect of RIP kinase deficiency on oxidative damage during retinal degeneration. Carbonyl formation is the most common products of protein oxidation. The retinal oxidative damage, as measured by ELISA for carbonyl content of proteins, was previously shown to increase in the period of cone degeneration in *rd10* mice (40). Consistent with this report, we found that the retinas of P35 *rd10* mice contained higher levels of carbonyl contents compared with WT retinas (Fig. S3). In contrast, *Rip3* deficiency significantly suppressed the increase of carbonyl contents in *rd10* mice (Fig. S3). These data demonstrate that RIP kinase regulates retinal oxidative damage in *rd10* mice.

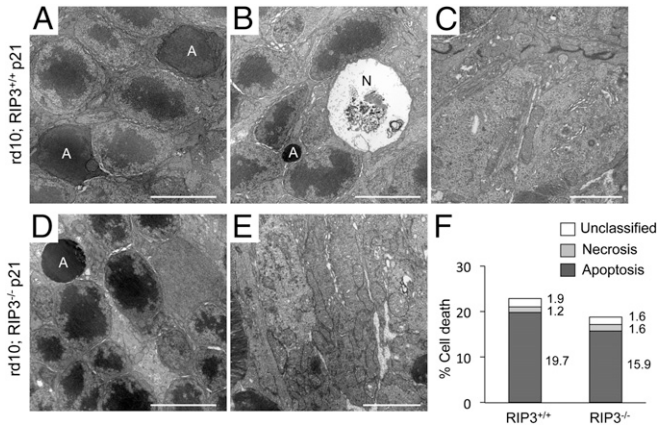

Fig. 3. Rod photoreceptor cell death is mainly associated with apoptotic morphology. (*A*–*E*) TEM photomicrographs in the ONL (*A*, *B*, and *D*) and in the inner segment (*C* and *E*) at P21 of *rd10*;*Rip3*$^{+/+}$ (*A*–*C*) and *rd10*;*Rip3*$^{-/-}$ mice (*D* and *E*). A, apoptotic cell; N, necrotic cell. [Scale bars, 5 μm (*A*, *B*, and *D*), 2 μm (*C* and *E*).] Apoptotic photoreceptor nuclei were frequently observed in both *rd10*;*Rip3*$^{+/+}$ (*A*) and *rd10*;*Rip3*$^{-/-}$ mice (*D*). Necrotic photoreceptor cell death was rarely seen (*B*). The mitochondrial structure was well preserved in both genotypes (*C* and *E*). (*F*) Quantification of apoptotic and necrotic photoreceptor cell death (n = 4 each). There was no significant difference in rod cell death morphology between *rd10*;*Rip3*$^{+/+}$ and *rd10*;*Rip3*$^{-/-}$ mice. The percentage of each cell death was shown on the right of bar.

Microglial Activation During Rod and Cone Cell Death in *Rd10* Mice. Dying cells, either through apoptosis or necrosis, expose and release several molecules that attract inflammatory cells (42). To assess the inflammatory response during rod and cone cell death in *rd10* mice, we performed immunofluorescence for the microglial marker Iba-1. Retinal flat mounts of WT and *Rip3*$^{-/-}$ mouse retinas showed similar density of ramified microglial cells in the outer plexiform layer (Fig. 7 *A*–*C*). In P25 *rd10* mouse retinas, activated amoeboid microglial cells with retracted processes and rounded cell bodies were substantially increased around the ONL, without any difference in the presence or absence of RIP3 (Fig. 7 *D*–*F*). Increased microglial infiltration was sustained at P42 and P56 *rd10* retinas, although the amoeboid microglia was relatively decreased (Fig. 7 *G* and *J*). In contrast, *rd10* mouse retinas lacking RIP3 showed significantly less microglial infiltration compared with control *rd10* mouse retinas at both P42 and P56 (P = 0.0374 each) (Fig. 7 *H*, *I*, *K*, and *L*). The microglial activation in *rd10*;*Rip3*$^{+/+}$ and *Rip3*$^{-/-}$ mouse retinas correlated well with the kinetics of rod and cone cell death in these animals. These findings suggest that RIP3 may not be essential for initiation of inflammation but it is required for maintenance of inflammation in *rd10* mice.

Discussion

In RP, most gene mutations identified are expressed exclusively in rod photoreceptors, yet cones that do not harbor gene abnormalities also die subsequent to the rod cell loss. Although rod cell death is caused by the deleterious gene mutations, it is puzzling why and how cones die in these diseases. Rod cell death in inherited retinal degeneration has been shown to occur through apoptosis (22, 38). In contrast, the mode of cone cell death has been relatively unexplored. In the present study, we showed that although rods die with apoptotic morphology, cone cell death is associated with necrotic features in *rd10* mice. Interestingly, in RP patient eyes with extensive rod degeneration, histological studies demonstrated that the remaining cones had swollen inner segments, vacuolated cytoplasm, and disruption of plasma membrane consistent with necrosis (43, 44). These morphological changes of cone photoreceptors were shown to be comparable in RP patients with different genetic mutations (45). Therefore, this finding implies that necrosis-mediating signaling may be the common mechanism underlying cone degeneration of RP. More importantly, we showed that genetic or pharmacologic inhibition of RIP kinase does not affect rod degeneration, but decreases necrotic

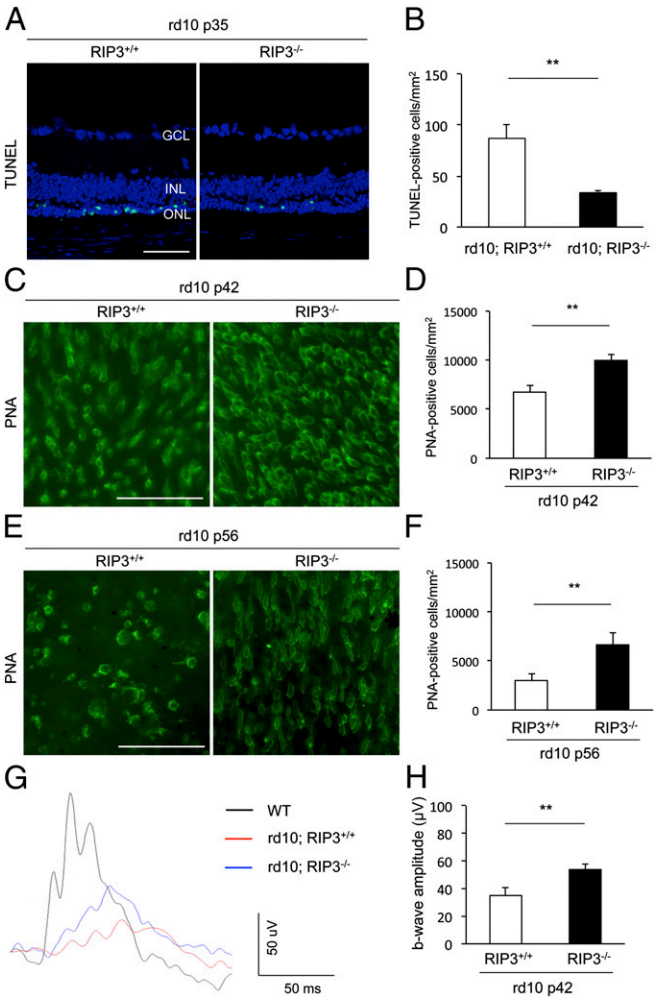

Fig. 4. *Rip3* deficiency decreases cone cell death and preserves cone function in *rd10* mice. (*A* and *B*) TUNEL staining (*A*) and quantification of TUNEL-positive photoreceptors (*B*) at P35 of *rd10;Rip3*$^{+/+}$ and *rd10;Rip3*$^{-/-}$ mice (n = 6 each). $^{**}P$ = 0.0062. GCL, ganglion cell layer; INL, inner nuclear layer; ONL, outer nuclear layer. (Scale bar, 50 μm.) (*C*–*F*) PNA staining (*C* and *E*) and quantification of PNA-positive cone photoreceptors (*D* and *F*) at P42 (*C* and *D*) and P56 (*E* and *F*) of *rd10;Rip3*$^{+/+}$ and *rd10;Rip3*$^{-/-}$ mice (n = 6 each). $^{**}P$ = 0.0039 each. (Scale bars, 50 μm.) *Rip3* deficiency decreased cone photoreceptor cell loss in *rd10* mice. (*G* and *H*) Photopic ERG (*G*) and quantification of b-wave amplitude (*H*) at P42 of *rd10;Rip3*$^{+/+}$ and *rd10;Rip3*$^{-/-}$ mice (n = 12 each). $^{**}P$ = 0.0022. The mean b-wave amplitude in *rd10;Rip3* $^{-/-}$ mice was significantly higher than those of *rd10;Rip3*$^{+/+}$ mice.

cone cell death and preserves their function. These results clearly demonstrate that distinct cell death mechanisms are involved in rod and cone degeneration, and suggest that RIP kinase may be a potential therapeutic target to protecting cones in inherited retinal degeneration.

Although the precise mechanisms by which RIP kinase induces necrosis remain unknown, several studies have demonstrated ROS overproduction as an important downstream event of RIP kinase activation (46, 47). Activated RIP3 interacts with metabolic enzymes, such as glycogen phosphorylase and glutamate-ammonia ligase, and thereby increases mitochondrial ROS production (12). On the other hand, RIP1 forms a complex with NADPH oxidase 1 and TNF-R1–associated death domain and produces superoxide, which in turn leads to induction of necrosis (41). In animal models of RP, Campochiaro and colleagues have demonstrated that retinal oxidative stress increases especially in the period of cone degeneration and that antioxidant treatments delay cone cell death (28, 40). However, the molecules that regulate ROS overproduction during cone degeneration were not identified. In this study, we found that *Rip3* deficiency suppresses the increase of retinal oxidative damage in *rd10* mice, suggesting that RIP kinase is partly responsible for ROS production in the phase of cone cell death.

Cell death and inflammation are interconnected (42). Dying cells expose or release numerous molecules to attract scavenger phagocytes; concomitantly, inflammation yields tissue damage and consequent cell death. In this study, we showed that *Rip3* deficiency reduced cone cell death and microglial activation in the period of cone degeneration in *rd10* mice. Although we cannot conclude which cells—cones or microglial cells—are primary targets of RIP3 inhibition, our time-course observation demonstrated no alteration in microglial response during rod degeneration in the presence or absence of RIP3, suggesting that RIP3 inhibition may target cones and suppress microglial activation that would otherwise occur subsequent to cone cell necrosis. This concept is supported by recent studies demonstrating that RIP kinase inhibition prevents intestinal cell necrosis and chronic inflammation induced by intestinal epithelium-specific knockout of Fas-associated death domain or caspase-8 (17, 18). However, as RIP3 is shown to directly activate inflammasome in macrophages (48), we cannot exclude the possibility that RIP3 modulates microglial function. Further studies using cone- or microglia-specific *Rip3* knockouts will be required to better understand the precise mechanisms by which RIP3 mediates cone necrosis and retinal inflammation in *rd10* mice.

Punzo et al. (29) recently reported the changes in the insulin/mammalian target of rapamycin pathway, which regulates cellular metabolism and autophagy, during cone degeneration. Indeed, our TEM analyses detected the formation of autophagic vacuoles in swollen cone photoreceptors in *rd10* mice (Fig. S4). These findings are consistent with previous histological studies of postmortem RP patient eyes describing the presence of autophagic vacuoles in remaining cones (43). Because excessive autophagy leads to cell death in some circumstances (49), autophagy may contribute to cone cell death in inherited retinal degeneration. Conversely, autophagy plays a prosurvival role via turnover of proteins, generation of nutrients, and elimination of damaged organelles (50). Therefore, autophagy may be activated as a consequence of necrotic disruption of organelles during cone degeneration. This idea is supported by a previous study showing

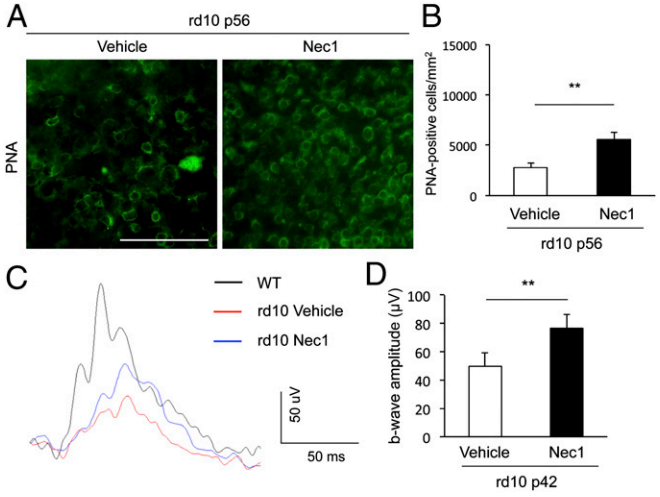

Fig. 5. RIP1 kinase inhibitor Nec-1 suppresses cone degeneration in *rd10* mice. (*A* and *B*) PNA staining (*A*) and quantification of PNA-positive cone photoreceptors (*B*) at P56 of *rd10* mice. The Alzet osmotic pumps containing Nec-1 (15 mg·kg·d, delivery for 28 d) or vehicle were implanted subcutaneously at P28 (n = 8 and 6). $^{**}P < 0.01$. (Scale bar, 50 μm.) (*C* and *D*) Photopic ERG (*C*) and quantification of b-wave amplitude (*D*) at P42 of *rd10* mice treated with Nec-1 or vehicle (n = 10 each). $^{**}P < 0.01$.

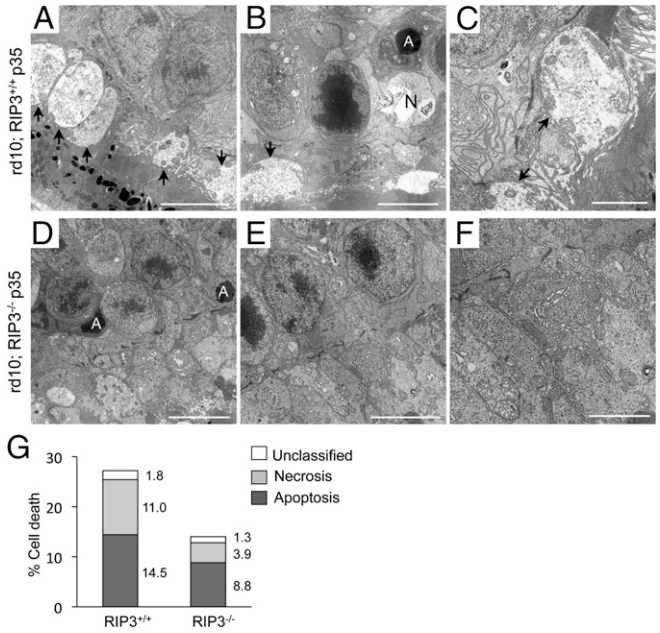

Fig. 6. Necrotic morphology of cone photoreceptor cell death in *rd10* mice. (*A–F*) TEM photomicrographs in the ONL and inner segment at P35 of *rd10;Rip3*$^{+/+}$ (*A–C*) and *rd10;Rip3*$^{-/-}$ (*D–F*) mice. A, apoptotic cell; N, necrotic cell. Arrow: cytoplasmic swelling of the inner segment. [Scale bar, 5 μm (*A*, *B*, *D* and *E*), 2 μm (*C* and *F*).] Cytoplasmic swelling of the inner segment and plasma membrane rupture were observed in *rd10;Rip3*$^{+/+}$ mice. The swelling of the cytoplasm and mitochondria was decreased in *rd10;Rip3*$^{-/-}$ mice. (*G*) Quantification of apoptotic and necrotic photoreceptor cell death (*rd10;Rip3*$^{+/+}$ mice: $n = 5$ and *rd10;Rip3*$^{-/-}$ mice: $n = 6$). The appearance of necrotic photoreceptors was significantly decreased in *rd10;Rip3*$^{-/-}$ mice ($P < 0.05$). The percentage of each cell death was shown on the right of bar.

that autophagy is induced during RIP kinase-mediated necrosis but is not critical for cell death (19). Defining the roles of autophagy in cone degeneration warrants further studies using genetic approaches, such as conditional knockout of autophagy-related genes in cone photoreceptors.

Whereas this study revealed an important role of RIP kinase in cone cell death of *rd10* mice, *Rip3* deficiency did not affect rod cell death even when combined with the pan-caspase inhibitor. These results differ from our previous study of retinal detachment models, which showed that *Rip3* deficiency leads to rod photoreceptor protection that is augmented by the pan-caspase inhibitor (21). This discrepancy may be attributed to different pathogenesis of retinal degeneration caused by genetic defects versus loss of nutrients in cells with normal genome function. Indeed, morphological features of rod cell death are different in these two models: although rod cell death in *rd10* mice is caused mostly by apoptosis, both apoptosis and necrosis are intermingled in retinal detachment (21, 51), supporting the idea that different molecules may be involved in each condition. Although rods undergo apoptosis in inherited retinal degeneration, previous studies have shown that caspase activation is not observed in *rd1* mice, which carry a viral insert and a nonsense mutation in exon 7 of the *Pde6β* gene (23). Taken together with our results, these data suggest that caspase and RIP kinase pathways may not be essential for rod cell death in RP models caused by *Pde6β* mutations. Interestingly, a recent study demonstrated a unique caspase-independent pathway of rod cell death in *rd1* mice, in which increased histone deacetylase activity leads to an activation of poly(ADP ribose) polymerase (52). Further studies will be needed to elucidate key molecules mediating rod cell death in inherited retinal degeneration. However, it should also be noted, that caspase inhibitors (zVAD and IDN), in contrast to necrostatins, have poor penetration through he blood-brain-barrier when administered systemically. In contrast to the previous study that the disease has a short time course and a single intravitreal administration is sufficient, this study required systemic month-long administration of the drugs. Thus, the negative results of this and other studies may be a technical one because of the limited permeability of caspase inhibitors through the blood-brain-barrier, leaving open the question of importance of caspase inhibition in rod cell death prevention.

Although loss of rod photoreceptors leads to night blindness, severe visual impairment is caused by the secondary death of cones that are responsible for central visual acuity, color vision, and loss of peripheral vision in patients with RP (1). Therefore, interventions to prevent or delay cone cell death will be critical to preserve the functional aspect of vision. Here, we demonstrate that in contrast to apoptotic rod cell loss, a necrotic mechanism involving RIP kinase is critical for induction of cone cell death in a mouse model of RP. In addition, pharmacologic or genetic inhibition of RIP kinase substantially prevents cone cell death

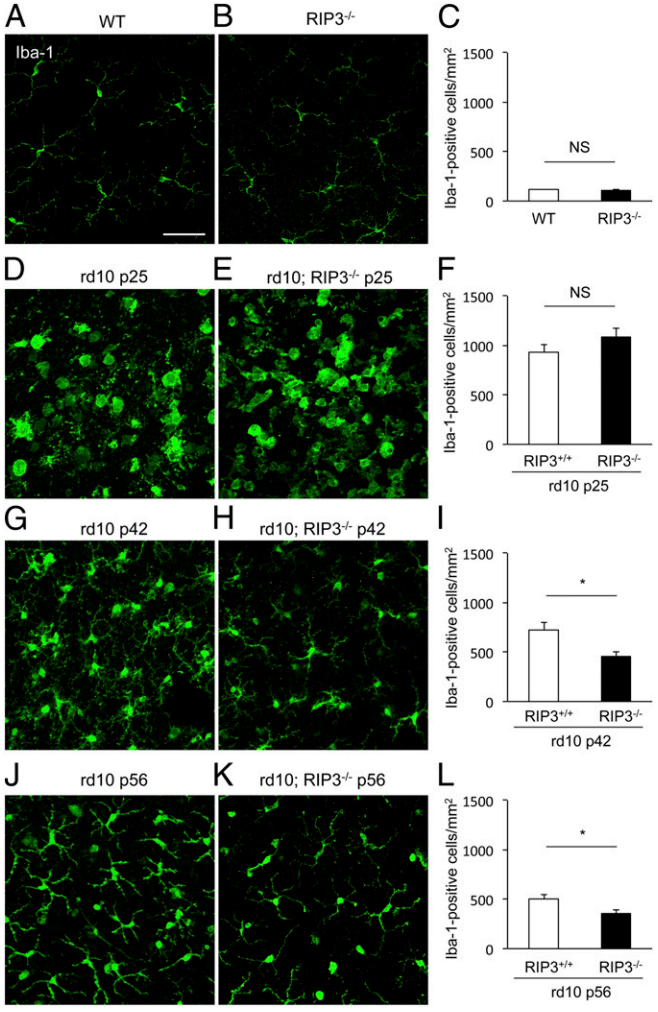

Fig. 7. Effect of RIP kinase on microglial activation during rod and cone cell death. (*A–I*) Immunofluorescence for Iba-1 (*A*, *B*, *D*, *E*, *G*, *H*, *J*, and *K*) and quantification of Iba-1^{+} microglia (*C*, *F*, *I*, and *L*) in WT (*A*), *Rip3*$^{-/-}$ (*B*), P25 *rd10;Rip3*$^{+/+}$ (*D*), P25 *rd10;Rip3*$^{-/-}$ (*E*), P42 *rd10;Rip3*$^{+/+}$ (*G*), P42 *rd10;Rip3*$^{-/-}$ (*H*), P56 *rd10;Rip3*$^{+/+}$ (*J*), and P56 *rd10;Rip3*$^{-/-}$ (*K*) mice ($n = 6$ each). *$P < 0.05$; NS, not significant. Whereas no difference in microglial activation was observed between P25 *rd10;Rip3*$^{+/+}$ and *rd10;Rip3*$^{-/-}$ mouse retinas (*F*), microglial infiltration was significantly reduced in *rd10;Rip3*$^{-/-}$ retinas compared with *rd10;Rip3*$^{+/+}$ retinas at both P42 and P56 (*I* and *L*). (Scale bar, 50 μm.)

and preserves their function, suggesting that RIP kinase may be a potential therapeutic target for patients with RP.

Materials and Methods

Animals. All animal experiments adhered to the statement of the Association for Research in Vision and Opthalmology. Protocols were approved by the Animal Care Committee of the Massachusetts Eye and Ear Infirmary. *Rd10* and WT C57BL/6 mice were purchased from The Jackson Laboratories. *Rip3*$^{-/-}$ mice were provided by Vishva M. Dixit (Genentech, San Francisco, CA) and backcrossed to C57BL/6 mice (33). *Rd10* mice were crossed with *Rip3*$^{-/-}$ mice, and the littermates from *rd10*;*Rip3*$^{+/-}$ males and *rd10*;*Rip3*$^{+/-}$ females were used for the experiments.

Nec-1 and the Pan-Caspase Inhibitor Treatment. Nec-1 was purchased from Sigma-Aldrich. The pan-caspase inhibitor IDN-6556 was prepared as previously described (53). To analyze the effects on rod cell death, the Alzet osmotic pumps (Model 1007D, duration 7 d) containing IDN-6556 (10 mg·kg·d), Nec-1 (15 mg·kg·d) plus IDN-6556 (10 mg·kg·d), or vehicle [50% (vol/vol) DMSO, 50% (vol/vol) PEG 400] were implanted subcutaneously at P21 of *rd10* mice. The effects of Nec-1 on cone cell death were examined by implantation of the Alzet osmotic pumps (Model 1004, duration 28 d) containing Nec-1 (15 mg·kg·d) or vehicle (50% DMSO, 50% PEG 400) at P28 of *rd10* mice.

Statistical Analysis. All values were expressed as the mean ± SEM. Statistical differences between two groups were analyzed by Mann–Whitney *U* test. Multiple group comparison was performed by ANOVA followed by Tukey–Kramer adjustments. Differences were considered significant at $P < 0.05$.

A detailed description of the methods is provided in *SI Materials and Methods*.

ACKNOWLEDGMENTS. We thank N. Michaud (Massachusetts Eye and Ear Infirmary) and F. Morikawa (Kyushu University) for technical assistance. This work was supported by the Research to Prevent Blindness Foundation Lions Eye Research Fund (to D.G.V.); Fight For Sight Grant in Aid (to D.G.V.); a Bausch & Lomb Vitreoretinal Fellowship (to H.M. and J.S.); and National Eye Institute Grant EY014104 (Massachusetts Eye and Ear Infirmary Core Grant).

1. Hartong DT, Berson EL, Dryja TP (2006) Retinitis pigmentosa. *Lancet* 368:1795–1809.
2. Berson EL, Rosner B, Sandberg MA, Weigel-Difranco C, Willett WC (2012) ω-3 Intake and visual acuity in patients with retinitis pigmentosa receiving vitamin A. *Arch Ophthalmol* 130:707–711.
3. Kerr JF, Wyllie AH, Currie AR (1972) Apoptosis: A basic biological phenomenon with wide-ranging implications in tissue kinetics. *Br J Cancer* 26:239–257.
4. Kroemer G, et al.; Nomenclature Committee on Cell Death 2009 (2009) Classification of cell death: Recommendations of the Nomenclature Committee on Cell Death 2009. *Cell Death Differ* 16:3–11.
5. Holler N, et al. (2000) Fas triggers an alternative, caspase-8-independent cell death pathway using the kinase RIP as effector molecule. *Nat Immunol* 1:489–495.
6. Matsumura H, et al. (2000) Necrotic death pathway in Fas receptor signaling. *J Cell Biol* 151:1247–1256.
7. Vandenabeele P, Galluzzi L, Vanden Berghe T, Kroemer G (2010) Molecular mechanisms of necroptosis: An ordered cellular explosion. *Nat Rev Mol Cell Biol* 11:700–714.
8. Micheau O, Tschopp J (2003) Induction of TNF receptor I-mediated apoptosis via two sequential signaling complexes. *Cell* 114:181–190.
9. Stanger BZ, Leder P, Lee TH, Kim E, Seed B (1995) RIP: A novel protein containing a death domain that interacts with Fas/APO-1 (CD95) in yeast and causes cell death. *Cell* 81:513–523.
10. Cho YS, et al. (2009) Phosphorylation-driven assembly of the RIP1-RIP3 complex regulates programmed necrosis and virus-induced inflammation. *Cell* 137:1112–1123.
11. He S, et al. (2009) Receptor interacting protein kinase-3 determines cellular necrotic response to TNF-alpha. *Cell* 137:1100–1111.
12. Zhang DW, et al. (2009) RIP3, an energy metabolism regulator that switches TNF-induced cell death from apoptosis to necrosis. *Science* 325:332–336.
13. Zhang H, et al. (2011) Functional complementation between FADD and RIP1 in embryos and lymphocytes. *Nature* 471:373–376.
14. Kaiser WJ, et al. (2011) RIP3 mediates the embryonic lethality of caspase-8-deficient mice. *Nature* 471:368–372.
15. Oberst A, et al. (2011) Catalytic activity of the caspase-8-FLIP(L) complex inhibits RIPK3-dependent necrosis. *Nature* 471:363–367.
16. Upton JW, Kaiser WJ, Mocarski ES (2010) Virus inhibition of RIP3-dependent necrosis. *Cell Host Microbe* 7:302–313.
17. Welz PS, et al. (2011) FADD prevents RIP3-mediated epithelial cell necrosis and chronic intestinal inflammation. *Nature* 477:330–334.
18. Günther C, et al. (2011) Caspase-8 regulates TNF-α-induced epithelial necroptosis and terminal ileitis. *Nature* 477:335–339.
19. Degterev A, et al. (2005) Chemical inhibitor of nonapoptotic cell death with therapeutic potential for ischemic brain injury. *Nat Chem Biol* 1:112–119.
20. Rosenbaum DM, et al. (2010) Necroptosis, a novel form of caspase-independent cell death, contributes to neuronal damage in a retinal ischemia-reperfusion injury model. *J Neurosci Res* 88:1569–1576.
21. Trichonas G, et al. (2010) Receptor interacting protein kinases mediate retinal detachment-induced photoreceptor necrosis and compensate for inhibition of apoptosis. *Proc Natl Acad Sci USA* 107:21695–21700.
22. Chang GQ, Hao Y, Wong F (1993) Apoptosis: Final common pathway of photoreceptor death in rd, rds, and rhodopsin mutant mice. *Neuron* 11:595–605.
23. Doonan F, Donovan M, Cotter TG (2003) Caspase-independent photoreceptor apoptosis in mouse models of retinal degeneration. *J Neurosci* 23:5723–5731.
24. Zeiss CJ, Neal J, Johnson EA (2004) Caspase-3 in postnatal retinal development and degeneration. *Invest Ophthalmol Vis Sci* 45:964–970.
25. Sanges D, Comitato A, Tammaro R, Marigo V (2006) Apoptosis in retinal degeneration involves cross-talk between apoptosis-inducing factor (AIF) and caspase-12 and is blocked by calpain inhibitors. *Proc Natl Acad Sci USA* 103:17366–17371.
26. Paquet-Durand F, et al. (2007) Excessive activation of poly(ADP-ribose) polymerase contributes to inherited photoreceptor degeneration in the retinal degeneration 1 mouse. *J Neurosci* 27:10311–10319.
27. Léveillard T, et al. (2004) Identification and characterization of rod-derived cone viability factor. *Nat Genet* 36:755–759.
28. Komeima K, Rogers BS, Lu L, Campochiaro PA (2006) Antioxidants reduce cone cell death in a model of retinitis pigmentosa. *Proc Natl Acad Sci USA* 103:11300–11305.
29. Punzo C, Kornacker K, Cepko CL (2009) Stimulation of the insulin/mTOR pathway delays cone death in a mouse model of retinitis pigmentosa. *Nat Neurosci* 12:44–52.
30. Chang B, et al. (2002) Retinal degeneration mutants in the mouse. *Vision Res* 42:517–525.
31. McLaughlin ME, Sandberg MA, Berson EL, Dryja TP (1993) Recessive mutations in the gene encoding the beta-subunit of rod phosphodiesterase in patients with retinitis pigmentosa. *Nat Genet* 4:130–134.
32. Usui S, et al. (2009) Increased expression of catalase and superoxide dismutase 2 reduces cone cell death in retinitis pigmentosa. *Mol Ther* 17:778–786.
33. Newton K, Sun X, Dixit VM (2004) Kinase RIP3 is dispensable for normal NF-kappa Bs, signaling by the B-cell and T-cell receptors, tumor necrosis factor receptor 1, and Toll-like receptors 2 and 4. *Mol Cell Biol* 24:1464–1469.
34. Feoktistova M, et al. (2011) cIAPs block Ripoptosome formation, a RIP1/caspase-8 containing intracellular cell death complex differentially regulated by cFLIP isoforms. *Mol Cell* 43:449–463.
35. Degterev A, et al. (2008) Identification of RIP1 kinase as a specific cellular target of necrostatins. *Nat Chem Biol* 4:313–321.
36. Grasl-Kraupp B, et al. (1995) In situ detection of fragmented DNA (TUNEL assay) fails to discriminate among apoptosis, necrosis, and autolytic cell death: A cautionary note. *Hepatology* 21:1465–1468.
37. Artus C, et al. (2010) AIF promotes chromatinolysis and caspase-independent programmed necrosis by interacting with histone H2AX. *EMBO J* 29:1585–1599.
38. Portera-Cailliau C, Sung CH, Nathans J, Adler R (1994) Apoptotic photoreceptor cell death in mouse models of retinitis pigmentosa. *Proc Natl Acad Sci USA* 91:974–978.
39. Blanks JC, Johnson LV (1984) Specific binding of peanut lectin to a class of retinal photoreceptor cells. A species comparison. *Invest Ophthalmol Vis Sci* 25:546–557.
40. Lee SY, et al. (2011) N-Acetylcysteine promotes long-term survival of cones in a model of retinitis pigmentosa. *J Cell Physiol* 226:1843–1849.
41. Kim YS, Morgan MJ, Choksi S, Liu ZG (2007) TNF-induced activation of the Nox1 NADPH oxidase and its role in the induction of necrotic cell death. *Mol Cell* 26:675–687.
42. Zitvogel L, Kepp O, Kroemer G (2010) Decoding cell death signals in inflammation and immunity. *Cell* 140:798–804.
43. Szamier RB, Berson EL (1982) Histopathologic study of an unusual form of retinitis pigmentosa. *Invest Ophthalmol Vis Sci* 22:559–570.
44. Szamier RB, Berson EL, Klein R, Meyers S (1979) Sex-linked retinitis pigmentosa: Ultrastructure of photoreceptors and pigment epithelium. *Invest Ophthalmol Vis Sci* 18:145–160.
45. To K, Adamian M, Berson EL (2004) Histologic study of retinitis pigmentosa due to a mutation in the RP13 gene (PRPC8): Comparison with rhodopsin Pro23His, Cys110Arg, and Glu181Lys. *Am J Ophthalmol* 137:946–948.
46. Lin Y, et al. (2004) Tumor necrosis factor-induced nonapoptotic cell death requires receptor-interacting protein-mediated cellular reactive oxygen species accumulation. *J Biol Chem* 279:10822–10828.
47. Vanlangenakker N, et al. (2011) cIAP1 and TAK1 protect cells from TNF-induced necrosis by preventing RIP1/RIP3-dependent reactive oxygen species production. *Cell Death Differ* 18:656–665.
48. Vince JE, et al. (2012) Inhibitor of apoptosis proteins limit RIP3 kinase-dependent interleukin-1 activation. *Immunity* 36:215–227.
49. Yu L, et al. (2004) Regulation of an ATG7-beclin 1 program of autophagic cell death by caspase-8. *Science* 304:1500–1502.
50. Mizushima N, Levine B (2010) Autophagy in mammalian development and differentiation. *Nat Cell Biol* 12:823–830.
51. Erickson PA, Fisher SK, Anderson DH, Stern WH, Borgula GA (1983) Retinal detachment in the cat: The outer nuclear and outer plexiform layers. *Invest Ophthalmol Vis Sci* 24:927–942.
52. Sancho-Pelluz J, et al. (2010) Excessive HDAC activation is critical for neurodegeneration in the rd1 mouse. *Cell Death Dis* 1:e24.
53. Hoglen NC, et al. (2004) Characterization of IDN-6556 (3-[2-(2-tert-butyl-phenylaminooxalyl)-amino]-propionylamino]-4-oxo-5-(2,3,5,6-tetrafluoro-phenoxy)-pentanoic acid): A liver-targeted caspase inhibitor. *J Pharmacol Exp Ther* 309:634–640.

Supporting Information

Murakami et al. 10.1073/pnas.1206937109

SI Materials and Methods

Animal Genotyping. *Rd10* mutation in exon 13 of the *Pde6β* gene [CGC (Arg) → TGC (Cys)] was identified by PCR using the forward primer 5′-TCTCAGAACCCACATGTACT-3′ and reverse primer 5′-TGATTCATCTAGCCCATCC-3′ and subsequent direct sequencing. The receptor-interacting protein 3 (*Rip3*) genotypes were analyzed by PCR using previously described primers (1).

RNA Extraction, RT-PCR, and Quantitative Real-Time PCR. Total RNA extraction and reverse transcription were performed as previously reported (2). A real-time PCR assay was performed with Prism 7700 Sequence Detection System (Applied Biosystems). TaqMan Gene Expression assays were used to check the expression of RIP3 (Mm00444947_m1) and RIP1 (Mm00436354_m1). For relative comparison of each gene, we analyzed the Ct value of real-time PCR data with the ΔΔCt method normalizing by an endogenous control (β-actin; Mm00607939_s1).

Western Blotting. The retinas of mice were collected and lysed in lysis buffer [50 mM Tris-HCl (pH 8), 120 mM NaCl and 1% Nonidet P-40, supplemented with a mixture of protein inhibitors (Roche Diagnostics)]. Samples were run on 4–12% SDS-PAGE and transferred onto PVDF membrane. After blocking with blocking buffer (Thermo Scientific), the membrane was reacted with RIP3 (1:10,000; Sigma) or RIP1 (1:2,000; BD Biosciences) antibody. They were then developed with enhanced chemiluminescence. Lane-loading differences were normalized by β-tubulin (1:1,000; Cell Signaling).

Iba-1 Staining. The neuroretinas were blocked with 3% nonfat dried milk and 0.3% triton X in PBS for 1 h, and incubated with anti–Iba-1 antibody (1:300; Wako) at 4 °C overnight. Anti-rabbit Alexa Fluor 488 (Invitrogen) was used as a secondary antibody. The neuroretinas were examined by Leica SP2 confocal microscopy.

ELISA. The amount of carbonyl adducts of proteins in retinal extract were determined with ELISA kits for protein carbonyls (Cell Biolabs) according to the manufacturer's instructions.

Electroretinogram. Photopic electroretinogram (ERG) was recorded using an Ocuscience HMsERG (Rolla, MO). Mice were anesthetized with an intrperitoneal injection of ketamine (100 mg/kg) and xylazine (10 mg/kg), pupils were dilated with 0.5% tropicamide and 0.5% phenylephrine hydrochloride, and the cornea was locally anesthetized with oxbuprocaine application. Body temperature was maintained at 37 °C with a heating pad. Silver-embedded thread eye electrodes were positioned across the apex of each cornea and held in place with 2.0% methylcellulose and optically clear mini-contact lens. Stainless steel needle reference electrodes were placed subcutaneously into the forehead, and a ground electrode was inserted into the base of the tail. Mice were adapted for 10 min to a background of white light at an intensity of 30 cd/m^2. Thirty-two photopic flashes were taken at 2 cd·s/m^2 and averaged.

Transmission Electron Microscopy. The eyes were enucleated, and the posterior segments were fixed in 2.5% glutaraldehyde and 2% paraformaldehyde in 0.1 M cacodylate buffer with 0.08 M $CaCl_2$ at 4 °C. The sections of retinas, retinal pigment epithelium, and choroid complexes were postfixed for 1.5 h in 2% aqueous OsO_4, dehydrated in ethanol and water, and embedded in EPON. Ultrathin sections were cut from blocks and stained with saturated aqueous uranyl acetate and Sato's lead stain. The specimens were observed with Philips CM10 electron microscope. Over 200 photoreceptors per eye were photographed and subjected to quantification of cell-death modes in a masked fashion. Photoreceptors showing cellular shrinkage and nuclear condensation were defined as apoptotic cells; photoreceptors associated with cellular and organelle swelling and discontinuities in plasma and nuclear membrane were defined as necrotic cells. Electron-dense granular materials were labeled simply as end-stage cell death/unclassified, because these materials are reported to occur subsequent to both apoptotic and necrotic cell death (3, 4).

Autophagosomes/autolysosomes were defined as membrane-bound compartments that contain cytoplasmic material or organelles, as previously described (5). Autophagosome was defined as a double- or multimembraned sturucture containing undigested cytoplasmic contents. Autolysosome contained degraded cytoplasmic material with increased electron density.

Peanut Agglutinin Staining. Eyes were enucleated and fixed in 4% PFA for 1 h. After washing with PBS, the neuroretinas were dissected, were blocked with 10% nonfat dried milk and 0.3% triton X in PBS for 1 h, and were incubated with FITC-conjugated peanut agglutinin (PNA) (1:100; Sigma-Aldrich) at 4 °C overnight. The neuroretinas were examined with a Zeiss Observer.Z1 microscope. The number of cones was determined as previously described (6). The retinal areas of 0.12 mm^2 located 0.5 mm superior, inferior, temporal, and nasal to the center of the optic nerve were photographed, and the number of PNA-positive cells in the four regions were counted using ImageJ software and averaged.

TUNEL Staining. TUNEL procedure and quantification of TUNEL-positive cells were performed using an ApopTag Fluorescein Direct in Situ Apoptosis Detection Kit (Millipore) according to the instructions of the manufacturer. Five sections were randomly selected in each eye. The midperipheral retinas in the nasal and temporal hemisphere were photographed, and the number of TUNEL-positive cells in the outer nuclear layer (ONL) was counted by masked observers. The retinal area was measured by ImageJ software. The data are expressed as TUNEL-positive cells per square millimeter of retinal area.

1. Newton K, Sun X, Dixit VM (2004) Kinase RIP3 is dispensable for normal NF-kappa Bs, signaling by the B-cell and T-cell receptors, tumor necrosis factor receptor 1, and Toll-like receptors 2 and 4. *Mol Cell Biol* 24:1464–1469.
2. Trichonas G, et al. (2010) Receptor interacting protein kinases mediate retinal detachment-induced photoreceptor necrosis and compensate for inhibition of apoptosis. *Proc Natl Acad Sci USA* 107:21695–21700.
3. Erickson PA, Fisher SK, Anderson DH, Stern WH, Borgula GA (1983) Retinal detachment in the cat: the outer nuclear and outer plexiform layers. *Investigative ophthalmology and visual science* 24:927–942.
4. Hisatomi T, et al. (2003) Clearance of apoptotic photoreceptors: elimination of apoptotic debris into the subretinal space and macrophage-mediated phagocytosis via phosphatidylserine receptor and integrin alphavbeta3. *Am J Pathol* 162:1869–1879.
5. Eskelinen EL (2008) To be or not to be? Examples of incorrect identification of autophagic compartments in conventional transmission electron microscopy of mammalian cells. *Autophagy* 4:257–260.
6. Usui S, et al. (2009) Increased expression of catalase and superoxide dismutase 2 reduces cone cell death in retinitis pigmentosa. *Mol Ther* 17:778–786.

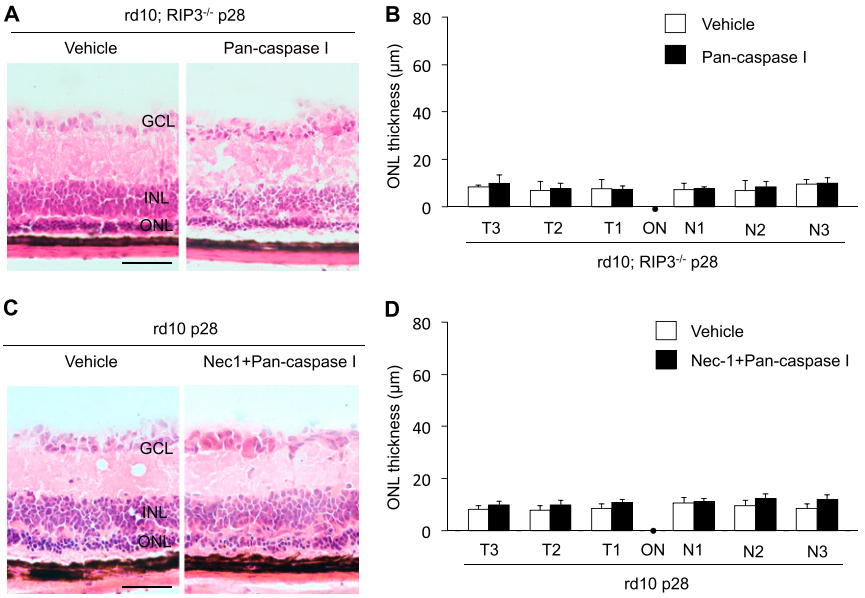

Fig. S1. Combined treatment with RIP kinase inhibition and the pan-caspase inhibitor does not affect rod degeneration in *rd10* mice. (*A* and *B*) Retinal histology (*A*) and quantification of ONL thickness (*B*) at postnatal day 28 (P28) of *rd10*;*Rip3*$^{-/-}$ mice treated with vehicle or the pan-caspase inhibitor IDN-6556 (n = 5 each). (Scale bar, 50 μm.) *Rd10*;*Rip3*$^{-/-}$ mice received subcutaneous implantation of the Alzet osmotic pump containing IDN-6556 (10 mg·kg·d, delivery for 7 d) or vehicle at p21. No significant difference in rod cell loss was observed by treatment with the pan-caspase inhibitor. (*C* and *D*) Retinal histology (*C*) and quantification of ONL thickness (*D*) at P28 of *rd10* mice treated with vehicle or necrostatin-1 (Nec-1) plus IDN-6556 (n = 8 each). (Scale bar, 50 μm.) *Rd10* mice received subcutaneous implantation of the Alzet osmotic pump containing Nec-1 (15 mg·kg·d) plus IDN-6556 (10 mg·kg·d) or vehicle at p21. There was no significant difference in rod cell loss between treatment with vehicle and Nec-1 plus IDN-6556.

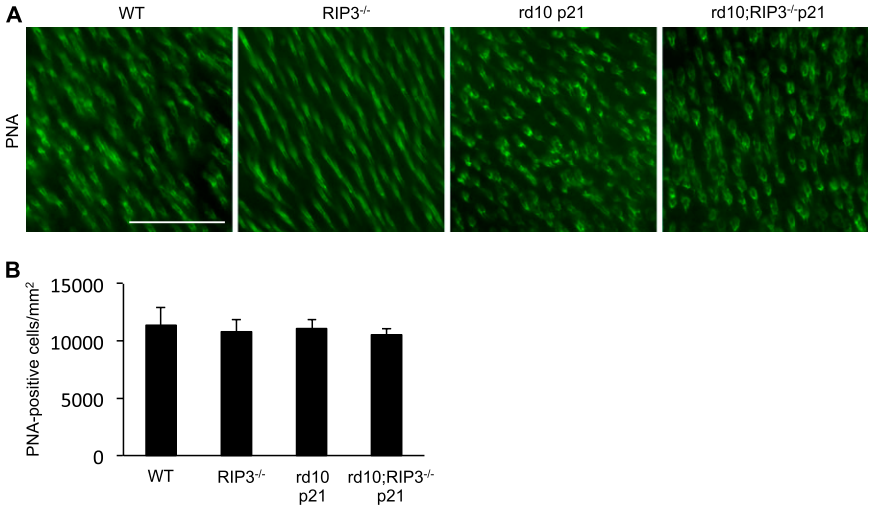

Fig. S2. Cone photoreceptor density in the phase of rod degeneration. PNA staining (*A*) and quantification of PNA-positive cone photoreceptors (*B*) at P21 of *rd10*;*Rip3*$^{+/+}$ and *rd10*;*Rip3*$^{-/-}$ mice. The retinas of WT and *Rip3*$^{-/-}$ mice were used as a control (n = 4 each). (Scale bar, 50 μm.) No significant difference in cone cell density was observed at this time point.

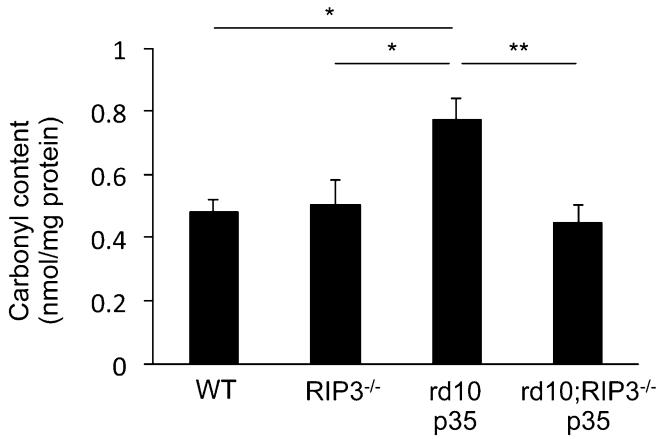

Fig. S3. RIP3 regulates retinal oxidative damage in *rd10* mice. ELISA to detect carbonyl contents in the retinas of P35 *rd10;Rip3*$^{+/+}$ and *rd10;Rip3*$^{-/-}$ mice (n = 8 each). The retinas of WT and *Rip3*$^{-/-}$ mice were used as controls (n = 7 and 8). *P < 0.05; **P < 0.01. *Rip3* deficiency reduced the increase of retinal oxidative damage in *rd10* mice.

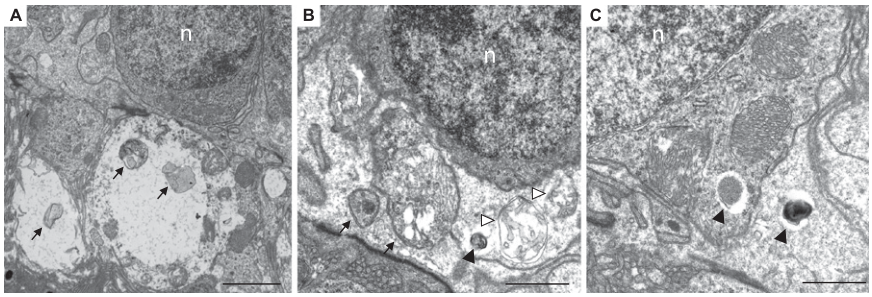

Fig. S4. Autophagy formation in the phase of cone cell death in *rd10* mice. Transmission electron microscopy photomicrographs in the ONL and inner segment in P35 *rd10* mouse retinas. Autophagosome (arrow) and autolysosomes (arrowhead) were frequently observed in the swollen cone photoreceptor cytoplasm. Some mitochondria were swollen and disrupted (white arrowhead). [Scale bar, 2 μm (*A*), 1 μm (*B* and *C*).]